CONTRACTILE SMOOTH MUSCLE AND ACTIVE STRESS GENERATION IN PORCINE COMMON CAROTIDS

Boran Zhou[1], David A. Prim[2], Eva J. Romito[2,3], Liam P. McNamara[2],

Francis G. Spinale[3,4], Tarek Shazly[2,5], John F. Eberth[2,4]

[1]Department of Radiology
Mayo Clinic College of Medicine
Rochester, MN, 55905.

[2]College of Engineering and Computing, Biomedical Engineering Program
University of South Carolina
Columbia, SC, 29208

[3]Cardiovascular Translational Research Center
University of South Carolina,
Columbia, SC, 29208

[4]School of Medicine, Department of Cell Biology and Anatomy
University of South Carolina
Columbia, SC, 29208

[5]College of Engineering and Computing, Department of Mechanical Engineering
University of South Carolina
Columbia, SC, 29208

Corresponding author:

John F. Eberth, Ph.D.
Email: john.eberth@uscmed.sc.edu
Address: USC SOM CBA, Bldg.1, Rm. C-36
Columbia, South Carolina, 29208

ABSTRACT

The mechanical response of intact blood vessels to applied loads can be delineated into passive and active components using an isometric decomposition approach. Whereas the passive response is due predominantly to the extracellular matrix (ECM) proteins and amorphous ground substance, the active response depends on the presence of smooth muscle cells (SMCs) and the contractile machinery activated within those cells. To better understand determinants of active stress generation within the vascular wall we subjected porcine common carotid arteries (CCAs) to biaxial inflation-extension testing under maximally contracted or passive SMC conditions and semi-quantitatively measured two known markers of the contractile SMC phenotype: smoothelin and smooth muscle-myosin heavy chain (SM-MHC). Using isometric decomposition and established constitutive models, an intuitive but novel correlation between the magnitude of active stress generation and the relative abundance of smoothelin and SM-MHC emerged. Our results reiterated the importance of stretch-dependent active stress generation to the total mechanical response. Overall these findings can be used to decouple the mechanical contribution of SMCs from the ECM and is therefore a powerful tool in the analysis of disease states and potential therapies especially where both constituent are altered.

Key words: Arterial mechanics; Biaxial active response; Active stress; Smooth muscle cells (SMC); Common carotid artery (CCA)

Word Count: 1,723 text + 750 images/tables = 2,473 words

INTRODUCTION

The passive mechanical response of blood vessels undergoing inflation-extension testing demonstrates a non-linear stress-stretch relationship due to the heterogeneous nature and inherent undulation of existing ECM proteins. Whereas these mechanics have been effectively modeled within the framework of nonlinear finite elasticity via biaxial mechanical testing, quantitative histology, and the subsequent identification of constitutive mechanical properties; studies of the active mechanical response have been fundamentally different. The most common approach being empirical identification of active stress-strain relations when SMCs are stimulated to contract [1,2].

Acute chemomechanical stimuli are capable of triggering vascular SMCs to initiate their contractile state in-vivo, resulting in a change in vessel geometry (lumen constriction or dilation). Although the majority of SMCs in the healthy vascular wall are of the contractile phenotype, SMCs are capable of modulating towards a synthetic or proliferative status commonly observed in carotid artery disease. This modulation dramatically affects the capacity of SMCs to generate active stresses and modify vascular tone [3]. There are surprisingly few studies, focused on the correlation between the prevalence of contractile SMC markers and the resultant isometric active stress generation [4,5]. The aims of this study are two-fold. First, an integrated experimental-theoretical approach was utilized to assess the passive and active biaxial mechanical responses of CCAs and identify a structure-motivated constitutive formulation for these tissues [6–9]. Second, semi-quantitative histology was performed to enable correlation

between the contractile SMC content and active circumferential stress in set of CCAs that were stimulated to maximally contract.

MATERIALS AND METHODS

Vessel isolation and biomechanical testing

All animal procedures were approved by the Institute Animal Care and Use Committee at the University of South Carolina. Adult male Yorkshire pigs weighing approximately 25 kg (8 weeks old, n=6) were anesthetized with sodium pentobarbital and CCAs isolated and dissected from perivascular tissue. Prior to and after excision, the distances between the proximal and distal ends of the vessel were measured and recorded using a digital caliper. Arteries were then gently rinsed and cannulated within the Bose BioDynamic 5270 mechanical testing device using a sterile 4-0 suture. The samples were submerged in and perfused with continuously aerated (95% O_2 + 5%CO_2) Krebs-Henseleit solution at 37°C and pH of 7.4. The maximal contracted state was induced by adding 10^{-5} M epinephrine to the circulating medium followed by a 15 min acclimation period [4]. Then samples underwent 5 cycles of biaxial mechanical preconditioning. Following preconditioning, blood vessels were quasi-statically pressurized (0 – 200 mmHg, 20 mmHg steps) over 3 cycles and at 3 levels of axial stretch spanning the in-situ axial stretch ratio, with the outer diameter and axial force recorded at each experimental state via integrated system components and software (Wintest 4.1, Bose ElectroForce, Eden Prairie, MN and Labview 2010, National Instruments Corporation, Austin, TX). To assess the mechanical response under fully-relaxed SMCs, the circulating medium was flushed and replaced with a 10^{-5} M sodium

nitroprusside solution. Following another 15 min acclimation period, identical mechanical preconditioning and biaxial mechanical testing protocols were repeated. Then ring slices were prepared (1 mm width) and a stress relieving cut introduced so that the thickness, opening angle and cross-sectional areas could be measured and calculated. The inner radii (r_i) at any deformed state could then be calculated from the incompressibility assumption.

Theoretical framework

CCAs are modeled as a cylindrically orthotropic, elastic, incompressible solid, under a state of axisymmetric deformation with the wall stress is divisible into active and passive components. Following a hybrid 2-D/3-D approach the constitutive relationships for the total stresses are defined by [4]:

$$\sigma_\theta^t = \sigma_r + \lambda_\theta \frac{\partial W}{\partial \lambda_\theta} + \sigma_\theta^a, \qquad \sigma_z^t = \sigma_r + \lambda_z \frac{\partial W}{\partial \lambda_z} + \sigma_z^a \ , \tag{1}$$

where the radial stress σ_r must be determined from the equilibrium and boundary conditions. Subscripts θ, r, and z indicate circumferential, radial, and axial directions, while t and a indicate the total and active stresses respectively. $W = W\left(\lambda_\theta, \lambda_z\right)$ is the strain energy function that characterizes the passive mechanical properties of the arterial wall.

We assume that the stress distributions across the wall are nearly uniform, and therefore mean stress and strain values adequately represent experimental states. Accordingly, hereafter stresses (and strains) refer to mean values calculated from experimental data using:

$$\sigma_r = -P\frac{r_i}{r_i + r_o}, \qquad \sigma_\theta = P\frac{r_i}{r_o - r_i}, \qquad \sigma_z = \frac{f}{\pi\left(r_o^2 - r_i^2\right)}, \tag{2}$$

where r_o is the deformed outer radius.

Active stresses are then computed via isometric comparisons between fully relaxed and maximally contracted SMC states. The active circumferential and axial stresses are therefore calculated as:

$$\sigma_\theta^a = \sigma_\theta^{ic} - \sigma_\theta^p + \sigma_r^p - \sigma_r^{ic}, \qquad \sigma_z^a = \sigma_z^{ic} - \sigma_z^p + \sigma_r^p - \sigma_r^{ic}, \tag{3}$$

where the superscript ic signifies the isometric contracted state and p the passive state. Therefore, combining equations (5) and (6), active stresses are directly calculated as

$$\sigma_\theta^a = \frac{2r_i r_o}{r_o^2 - r_i^2}\left(P_{ic} - P_p\right) \qquad \sigma_\theta^a = \frac{f_{ic} - f_p}{\pi\left(r_o^2 - r_i^2\right)} + \frac{r_i}{r_i + r_o}\left(P_{ic} - P_p\right) \tag{4}$$

where P_p and P_{ic} are the pressures and f_p and f_{ic} the forces in the passive and isometric contraction states, respectively.

The passive mechanical properties of CCAs were modelled via a structure-motivated strain energy function W [10]:

$$W = c\left(I_1 - 3\right) + \sum_{k=1,2,3,4} \frac{b_{1k}}{2b_{2k}}\left\{ \exp\left[b_{2k}\left(\lambda_k^2 - 1\right)^2 \right] - 1 \right\}. \tag{5}$$

The first term in W accounts for the isotropic contribution of elastin [11] with c a material constant and $I_1 = \lambda_\theta^2 + \lambda_z^2 + \left(\lambda_\theta \lambda_z\right)^{-2}$ the first invariant of the Cauchy-Green strain tensor. The second term includes the contribution of k (four) families of collagen fibers with a specific orientation angle α ; $b_{1k,}$ and b_{2k} are material constants; and

$\lambda_k = \sqrt{\lambda_\theta^2 sin^2\alpha_k + \lambda_z^2 cos^2\alpha_k}$ the stretch ratio experienced by each family of collagen fibers due to deformation. Unknown material constants are determined by minimization of the objective function

$$\Omega_p = \sum_{n=1}^{N}\left(\frac{\hat{\sigma}_{\theta n}^T - \hat{\sigma}_{\theta n}^E}{\hat{\sigma}_{\theta n}^E}\right)^2 + \sum_{n=1}^{N}\left(\frac{\hat{\sigma}_{zn}^T - \hat{\sigma}_{zn}^E}{\hat{\sigma}_{zn}^E}\right)^2, \tag{6}$$

where

$$\hat{\sigma}_\theta^E = P_p\frac{r_i}{r_o - r_i} + P_p\frac{r_i}{r_o + r_i}, \qquad \hat{\sigma}_z^E = \frac{f_p}{\pi\left(r_o^2 - r_i^2\right)} + P_p\frac{r_i}{r_o + r_i}, \tag{7}$$

and

$$\hat{\sigma}_\theta^T = \lambda_\theta\frac{\partial W}{\partial \lambda_\theta}, \quad \hat{\sigma}_z^T = \lambda_z\frac{\partial W}{\partial \lambda_z}. \tag{8}$$

Superscripts T and E refer to theoretical and experimental values, respectively.

Analytical form for the active stress-stretch relationship

We assume the active stress in the circumferential direction depends on stretch, i.e. $\sigma_\theta^a = \sigma_\theta^a\left(\lambda_\theta, \lambda_z\right)$, and apply the following constitutive relation:

$$\sigma_\theta^a = S_\theta\left(\alpha_\theta\lambda_z - 1\right)\lambda_\theta\left[1 - \left(\frac{\lambda_{\theta\max} - \lambda_\theta}{\lambda_{\theta\max} - \lambda_{\theta o}}\right)^2\right], \tag{9}$$

where S_θ is an activation parameter with units of stress; $\lambda_{\theta\max}$ is the stretch at which the maximal active circumferential stresses are developed; $\lambda_{\theta o}$ are the stretches below which no active stresses are generated; and α_θ is a material constant that relates the active stresses in the circumferential direction to axial stretches. Model parameterization was achieved via minimization of the objective function,

$$\Omega_\theta = \sum_{n=1}^{N} \left(\frac{\sigma_\theta^{a(theo)} - \sigma_\theta^{a(exp)}}{\sigma_\theta^{a(exp)}} \right)_n^2 \quad (10)$$

where $n = 1, 2, \ldots . N$ is the number of the experimental states. The resulting material constants and residuals for both minimization problems are reported in Tables 1-2.

Histological quantification

Specimens were fixed in 4% paraformaldehyde, embedded in paraffin blocks, and cut to approximately 5 *μm* sections using a microtome. Alternating sections were stained for Verhoeff's elastic fiber counterstained with methyl blue, Hematoxylin and Eosin (H&E), smoothelin, or smooth muscle-myosin heavy chain (SM-MHC). Mouse monoclonal anti-smoothelin antibody (R4A) and rabbit polyclonal anti-SM-MHC 11 antibody and were obtained from Abcam (Cambridge, MA). Antibodies were stained using a Dako (Carpinteria, CA) immune-peroxidase kit with 3,3'-diaminobenzidinetrahydrochloride (DAB) as the peroxidase substrate. All samples were stained together to prevent batch-to-batch variations and imaged under similar lighting conditions using a Nikon E600 microscope with CCD camera and computer interface with Q Capture (QImaging). Each slide (n=4 for each vessel) was imaged in at least 3 locations. Image thresholding was conducted to compare pixels stained positive for contractile SMCs – as represented by immuno-stained brown smoothelin or SM-MHC – to total tissue pixels from the H&E image using ImageJ software (National Institutes of Health) with the "Threshold_Colour" plugin (H=80-215^o, S=0.25-1.0, V=0.0-1.0). Each total tissue area was saved as a region of interest (ROI), which was then superimposed as an ROI on the corresponding IHC slides to estimate pixel area density (area positively stained pixels / area all tissue pixels) [12,13]. Protein analysis was performed

in this manner, rather than using a Western Blot, to identify spatial differences in organization of contractile markers and is supported by a number of prior studies [14–16].

RESULTS AND DISCUSSION

The aim of this study was to quantify the active and passive mechanical response of porcine CCAs to biaxial loading (Figure 1-2), to formulate constitutive equations for the mechanical properties of these arteries (Table 1-2), and evaluate the relationship between active stress generation and two histological markers of SMC phenotype: smoothelin and SM-MHC (Figure 3-4). A tremendous advantageous enabled by this approach is the capacity to isolate the passive (ECM based) from the active (contractile SMC based) contributions to the total stress state.

A spectrum of SMC phenotype exist in both the healthy and diseased vascular wall [3,17]. Two established markers used to indicate contractile phenotype are smoothelin and SM-MHC [18] while specific markers of synthetic/proliferative SMCs are more difficult to ascertain [19]. Smoothelin is expressed only by contractile SMCs, and plays a role in regulating and stabilizing contractile structures [17,20] while SM-MHC is directly involved in the process of contraction [3,18]. Other contractile markers such as alpha smooth muscle actin is less specific and found in other cell types. Although apparent in the reported specimen (Figure 3C&D) DAB staining intensity was not quantified as a separate variable. Instead pixels were simply considered as positively or negatively stained based on ranges determined by the thresholding analysis (see insets of Figure 3C&D) and reported as pixel/pixel density. Moreover, our findings yielded a

homogeneous distribution of these sub-cellular constituents within the media. Overall histological observations are within an acceptable range of other investigators using different analytical techniques. [21].

Polynomial regression was performed between active circumferential stress and smoothelin, or SM-MHC density (Figure 4) resulting in an excellent fit for both indicators of contractile phenotype. We acknowledge sample size limitations in the current study allow for the analysis to contain only 6 data points. Despite this, both phenotype markers suggest the capacity to generate active stress reaches a peak around 0.5 (pixel/pixel). We offer the following explanations for this behavior. (i) the physiological stretch conditions used for correlation may not be at the maxima, (ii) smoothelin and SM-MHC are markers of SMC phenotype but not of the actual contraction itself, (iii) the orientation of SMCs present are not aligned in the circumferential direction, or (iv) the matrix stiffness as it contracts. The latter is consistent with nonlinear theory of finite elasticity and represents a common behavior of soft biological materials.

CCAs generate active stresses lower than the physiologic passive stresses which is in contrast to, but a logical extension of the author's earlier work in muscular renal arteries [4]. Naturally the carotid artery studied here is of the elastic-type and therefor contains a greater proportion of extra-cellular-matrix proteins [22]. Nevertheless, vasomotor control of the CCA plays an important role in maintaining adequate perfusion to the head and neck while SMC contractile properties are essential in maintaining tissue homeostasis and is an important subject matter for an active vascular mechanics investigation.

CONCLUSION

Using an isometric decomposition approach the passive and active contributions to the total stress state of porcine CCAs have been delineated and the latter correlated with contractile SMC phenotype markers smoothelin and SM-MHC.

ACKNOWLEDGMENTS

The authors would like to acknowledge the funding sources for this work; NIH P20GM103499 (JFE, TS), R01HL222090 (FGS), and a Merit Award from the Veterans' Affairs Health Administration 2I01-BX000168 (FGS).

REFERENCES

[1] Cox, R. H., 1978, “Regional variation of series elasticity in canine arterial smooth muscles.,” Am. J. Physiol., **234**(18), pp. H542–H551.

[2] Dobrin, P. B., 1973, “Influence of initial length on length tension relationship of vascular smooth muscle,” Am. J. Physiol., **225**, pp. 664–670.

[3] Doran, A. C., Meller, N., and McNamara, C. A., 2008, “Role of Smooth Muscle Cells in the Initiation and Early Progression of Atherosclerosis,” Arterioscler. Thromb. Vasc. Biol. , **28**(5), pp. 812–819.

[4] Zhou, B., Rachev, A., and Shazly, T., 2015, “The biaxial active mechanical properties of the porcine primary renal artery.,” J. Mech. Behav. Biomed. Mater., **48**, pp. 28–37.

[5] Agianniotis, A., Rachev, A., and Stergiopulos, N., 2012, “Active axial stress in mouse aorta,” J. Biomech., **45**(11), pp. 1924–1927.

[6] Cox, R. H., 1975, “Arterial wall mechanics and composition and the effects of smooth muscle activation,” Am. J. Physiol. -- Leg. Content, **229**(3), pp. 807–812.

[7] Dobrin, P. B., 1973, “Isometric and isobaric contraction of carotid arterial smooth muscle,” Am. J. Physiol., **225**(3), pp. 659–663.

[8] Fridez, P., Makino, A., Kakoi, D., Miyazaki, H., Meister, J. J., Hayashi, K., and Stergiopulos, N., 2002, “Adaptation of conduit artery vascular smooth muscle tone to induced hypertension,” Ann. Biomed. Eng., **30**(7), pp. 905–916.

[9] Rachev, A., and Hayashi, K., 1999, “Theoretical Study of the Effects of Vascular Smooth Muscle Contraction on Strain and Stress Distributions in Arteries,” Ann. Biomed. Eng., **27**(4), pp. 459–468.

[10] Baek, S., Gleason, R. L., Rajagopal, K. R., and Humphrey, J. D., 2007, “Theory of small on large: potential utility in computations of fluid–solid interactions in arteries ,” Comput. Methods Appl. Mech. Eng., **196**(31–32), pp. 3070–3078.

[11] Zhou, B., Wolf, L., Rachev, A., and Shazly, T., 2013, “A structure-motivated model of the passive mechanical response of the primary porcine renal artery,” J. Mech. Med. Biol., **14**(3), p. 1450033.

[12] Taylor, C. R., and Levenson, R. M., 2006, “Quantification of immunohistochemistry—issues concerning methods, utility and semiquantitative assessment II,” Histopathology, **49**(4), pp. 411–424.

[13] Landini, G., 2008, “Advanced shape analysis with ImageJ,” ImageJ User and Developer Conference, Luxembourg.

[14] Nedorost, L., Uemura, H., Furck, A., Saeed, I., Slavik, Z., Kobr, J., and Tonar, Z., 2013, “Vascular Histopathologic Reaction to Pulmonary Artery Banding in an In Vivo Growing Porcine Model,” Pediatr. Cardiol., **34**(7), pp. 1652–1660.

[15] Fredersdorf, S., Thumann, C., Ulucan, C., Griese, D. P., Luchner, A., Riegger, G. A. J., Kromer, E. P., and Weil, J., 2004, “Myocardial hypertrophy and enhanced left ventricular contractility in Zucker diabetic fatty rats,” Cardiovasc. Pathol., **13**(1), pp. 11–19.

[16] Eberlov, L., Tonar, Z., Witter, K., Kkov, V., Nedorost, L., Koraben, M., Tolinger, P., Koov, J., Boudov, L., Teka, V., Houdek, K., Molek, J., Vrzalov, J., Peta, M., Topolan, O., and Valenta, J., 2012, “Asymptomatic abdominal aortic aneurysms show histological signs of progression: A quantitative histochemical analysis,” Pathobiology, **80**(1), pp. 11–23.

[17] van der Loop, F. T. L., Gabbiani, G., Kohnen, G., Ramaekers, F. C. S., and van Eys, G. J. J. M., 1997, “Differentiation of Smooth Muscle Cells in Human Blood Vessels as Defined by Smoothelin, a Novel Marker for the Contractile Phenotype,” Arterioscler. Thromb. Vasc. Biol. , **17**(4), pp. 665–671.

[18] Rensen, S. S. M., Doevendans, P. a F. M., and van Eys, G. J. J. M., 2007, “Regulation and characteristics of vascular smooth muscle cell phenotypic diversity.,” Neth. Heart J., **15**(3), pp. 100–108.

[19] Hao, H., Gabbiani, G., and Bochaton-Piallat, M.-L., 2003, “Arterial Smooth Muscle Cell Heterogeneity: Implications for Atherosclerosis and Restenosis Development ,” Arterioscler. Thromb. Vasc. Biol. , **23**(9), pp. 1510–1520.

[20] van Eys, G. J., Niessen, P. M., and Rensen, S. S., 2007, “Smoothelin in Vascular Smooth Muscle Cells,” Trends Cardiovasc. Med., **17**(1), pp. 26–30.

[21] Roy, S., Silacci, P., and Stergiopulos, N., 2005, “Biomechanical proprieties of decellularized porcine common carotid arteries,” Am. J. Physiol. - Hear. Circ. Physiol., **289**(4), pp. H1567–H1576.

[22] Berne, R. M., and Levy, M. N., 2001, Cardiovascular Physiology, Mosby, Inc., St. Louis, Missouri.

Figure and Table and Captions

Figure 1: Pressure-deformed outer diameter (left) and axial force-pressure (right) relationships for a representative porcine common carotid artery (Sample 1). The mechanical response was recorded under conditions of maximally contracted (•) and fully relaxed (◦) smooth muscle cell states, and at three axial stretch ratios (λ_z) that span the in-situ value. Error bars represent the standard deviation of three repeat measurements on the same vessel.

Figure 2: Representative (top) total stress after isometric contraction, (middle) passive stress and (bottom) active circumferential stress – stretch relationships for a porcine common carotid artery at three levels of axial stretch (Sample 1). Error bars represent the standard deviation of three repeat measurements on the same vessel. Data points indicate experimentally recorded values, while solid/dashed lines indicate theoretical predictions.

Figure 3: Representative histological images (Sample 2 in Tables 1-4), of the porcine common carotid arteries at 100x magnification; (A) Verhoeff's elastic fiber counterstained with methyl blue, (B) Hematoxylin and Eosin, (C) smoothelin DAB immunostaining with thresholded inset and, (D) smooth muscle-myosin heavy chain DAB immunostaining with thresholded inset.

Figure 4: Second order polynomial fit between the mean active circumferential stress (λ_θ =1.42, λ_z = 1.6) and smoothelin (•) and smooth muscle myosin heavy chain SM-MHC (×) density (area positively stained / area all tissue) content in the porcine common carotid arteries. Error bars ± STD mean.

Table 1. Best-fit parameters for the utilized structure-motivated strain energy function for the passive mechanical response.

Table 2. Best-fit parameters for the proposed model of the circumferential active stresses.

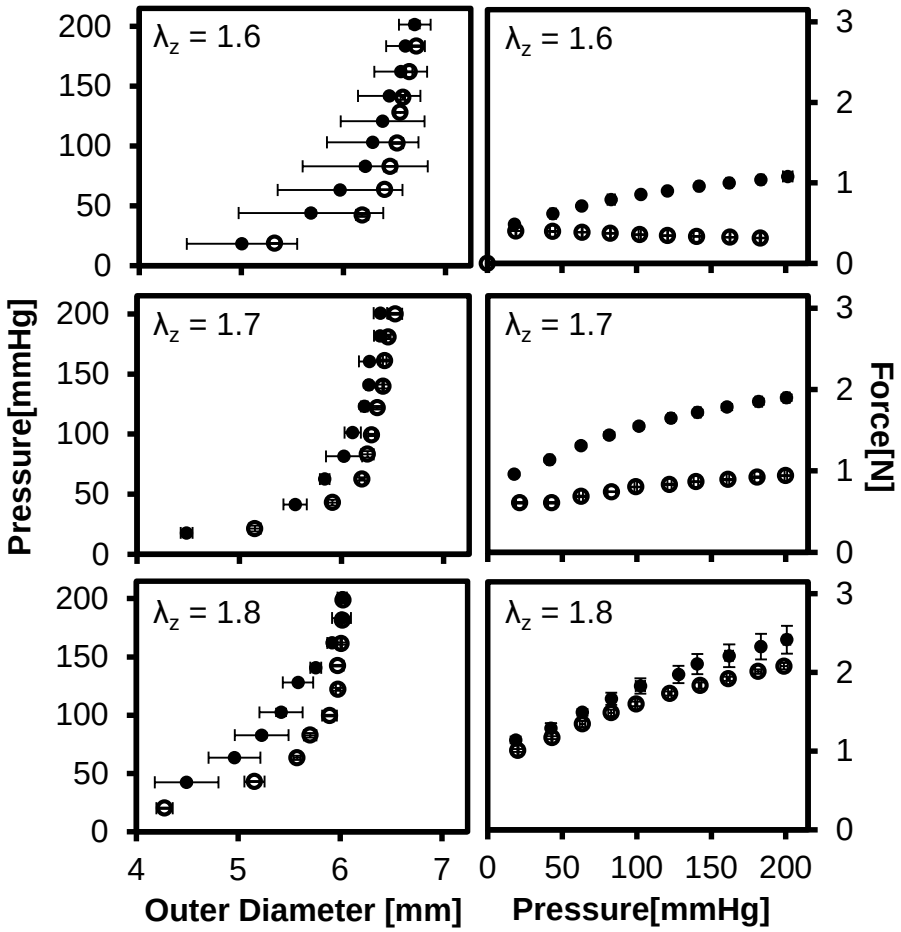

Figure 1: Pressure-deformed outer diameter (left) and axial force-pressure (right) relationships for a representative porcine common carotid artery (Sample 1). The mechanical response was recorded under conditions of maximally contracted (•) and fully relaxed (◦) smooth muscle cell states, and at three axial stretch ratios (λ_z) that span the in-situ value. Error bars represent the standard deviation of three repeat measurements on the same vessel.

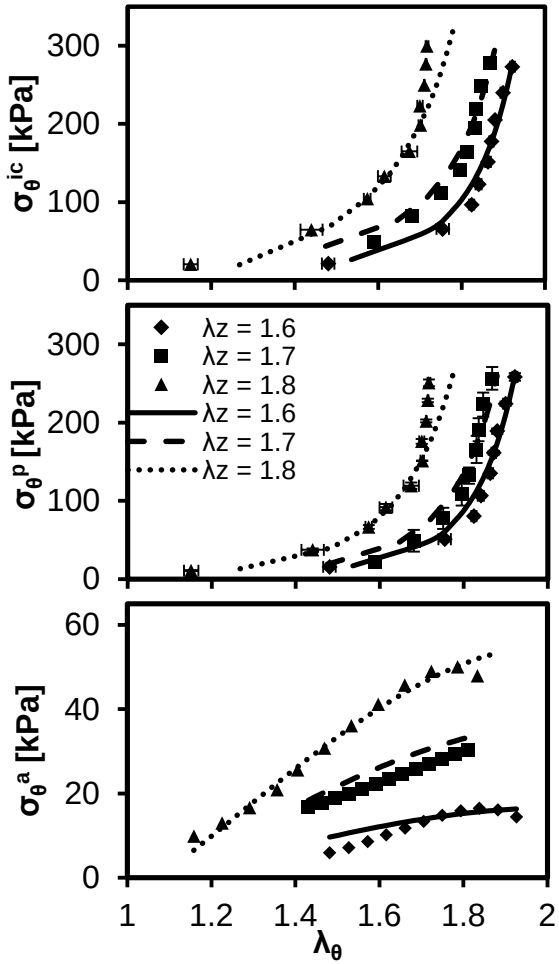

Figure 2: Representative (top) total stress after isometric contraction, (middle) passive stress and (bottom) active circumferential stress – stretch relationships for a porcine common carotid artery at three levels of axial stretch (Sample 1). Error bars represent the standard deviation of three repeat measurements on the same vessel. Data points indicate experimentally recorded values, while solid/dashed lines indicate theoretical predictions.

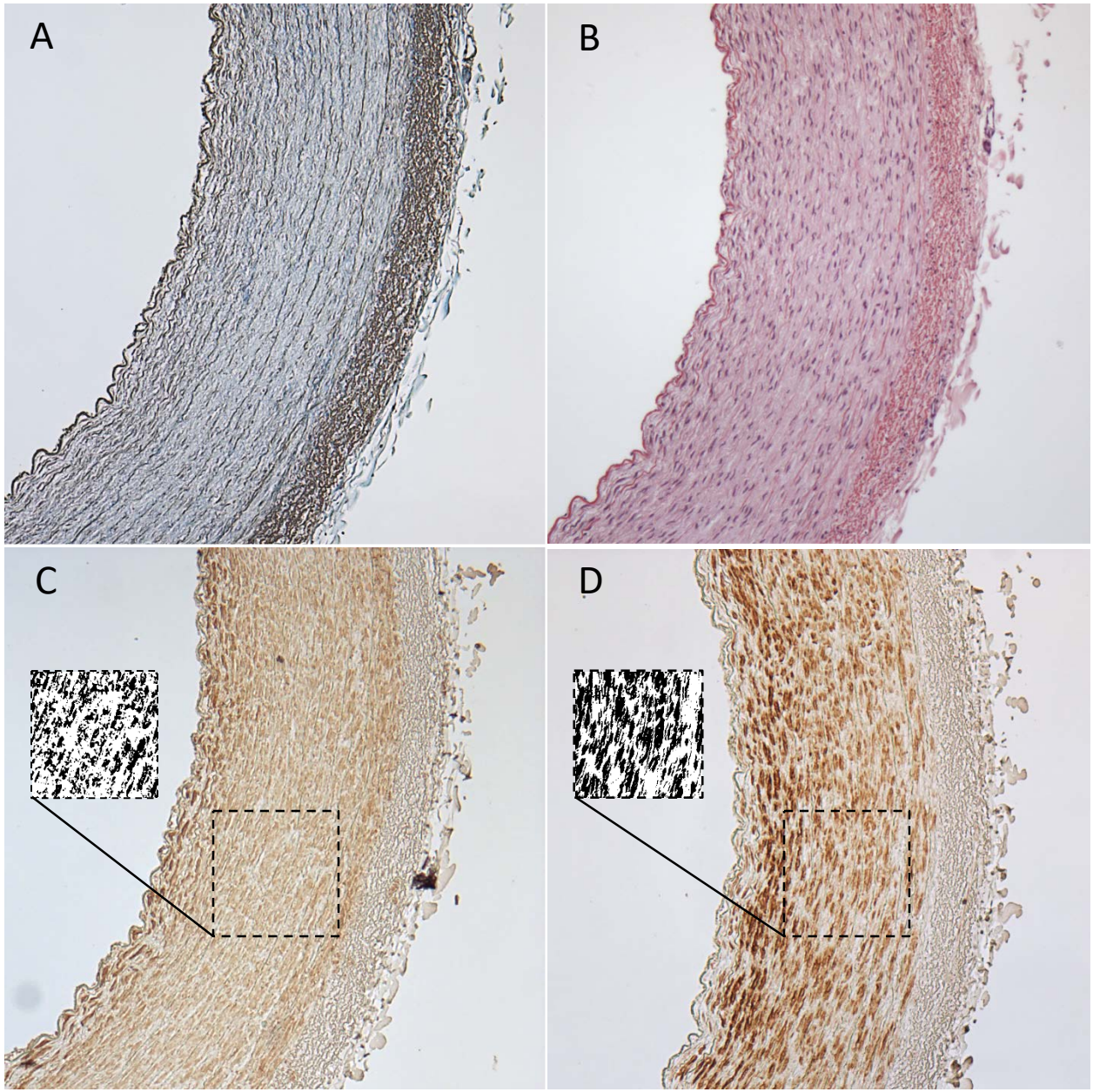

Figure 3: Representative histological images (Sample 2 in Tables 1-4), of the porcine common carotid arteries at 100x magnification; (A) Verhoeff's elastic fiber counterstained with methyl blue, (B) Hematoxylin and Eosin, (C) smoothelin DAB immunostaining with thresholded inset and, (D) smooth muscle-myosin heavy chain DAB immunostaining with thresholded inset.

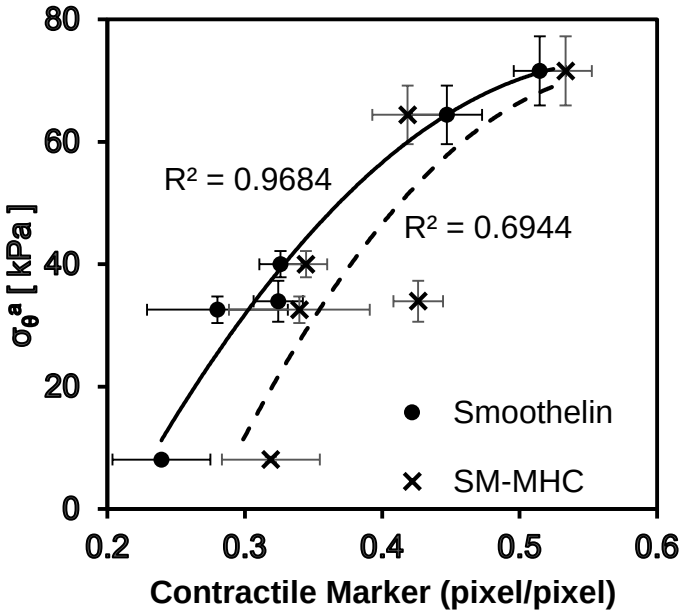

Figure 4: Second order polynomial fit between the mean active circumferential stress (λ_θ =1.42 , λ_z = 1.6) and smoothelin (•) and smooth muscle myosin heavy chain SM-MHC (×) density (area positively stained / area all tissue) content in the porcine common carotid arteries. Error bars ± STD mean.

Table 1. Best-fit parameters for the utilized structure-motivated strain energy function for the passive mechanical response.

Sample	c [Pa]	b_{11} [Pa]	b_{21}	b_{12} [Pa]	b_{22}	b_{13} [Pa]	b_{23}	alpha [°]	R^2
1	111.3	2179	0.2	1476.4	0.2	100.2	1.1	30.2	0.9
2	13793.0	10976	0.2	100.1	0.6	100.3	0.7	27.4	0.9
3	7680.7	215.1	0.4	1240.7	0.5	98.9	0.9	44.8	0.4
4	7166.4	506.6	1.3	5677.1	1.1	100.9	3.4	35.8	0.4
5	108.7	1691.2	0.5	1604.5	0.8	101.6	2.1	30.4	1.3
6	106	1028	0.58	630.09	1.45	101.3	2.16	35.62	0.73
Average	4827.68	2765.96	0.53	1788.13	0.76	100.53	1.74	34.03	0.78
SD	5176.77	3731.33	0.35	1814.09	0.40	0.88	0.91	5.67	0.32

Table 2. Best-fit parameters for the proposed model of the circumferential active stresses.

Sample	S_θ [kPa]	α_θ	$\lambda_{\theta,max}$	$\lambda_{\theta,0}$	R^2
1	150.50	0.66	1.87	1.08	0.98
2	54.76	0.83	1.59	0.89	0.77
3	73.35	0.76	1.95	1.09	0.83
4	94.81	1.90	2.58	0.83	0.61
5	31.72	2.01	1.79	1.19	0.75
6	24.82	2.00	1.98	1.33	0.68
Average	71.66	1.36	1.96	1.07	0.77
SD	42.48	0.61	0.31	0.17	0.12